Published online 25 February 2014 *Nucleic Acids Research, 2014, Vol. 42, No. 8* ***4985–4995***
doi:10.1093/nar/gku148

Reversible Top1 cleavage complexes are stabilized strand-specifically at the ribosomal replication fork barrier and contribute to ribosomal DNA stability

Claudia Krawczyk[1], Vincent Dion[2], Primo Schär[1,*] and Olivier Fritsch[1,*]

[1]Department of Biomedicine, University of Basel, 4058 Basel, Switzerland and [2]Friedrich Miescher Institute for Biomedical Research, Maulbeerstrasse 66, 4058 Basel, Switzerland

Received July 17, 2013; Revised January 14, 2014; Accepted January 31, 2014

ABSTRACT

Various topological constraints at the ribosomal DNA (rDNA) locus impose an extra challenge for transcription and DNA replication, generating constant torsional DNA stress. The topoisomerase Top1 is known to release such torsion by single-strand nicking and re-ligation in a process involving transient covalent Top1 cleavage complexes (Top1cc) with the nicked DNA. Here we show that Top1ccs, despite their usually transient nature, are specifically targeted to and stabilized at the ribosomal replication fork barrier (rRFB) of budding yeast, establishing a link with previously reported Top1 controlled nicks. Using ectopically engineered rRFBs, we establish that the rRFB sequence itself is sufficient for induction of DNA strand-specific and replication-independent Top1ccs. These Top1ccs accumulate only in the presence of Fob1 and Tof2, they are reversible as they are not subject to repair by Tdp1- or Mus81-dependent processes, and their presence correlates with Top1 provided rDNA stability. Notably, the targeted formation of these Top1ccs accounts for the previously reported broken replication forks at the rRFB. These findings implicate a novel and physiologically regulated mode of Top1 action, suggesting a mechanism by which Top1 is recruited to the rRFB and stabilized in a reversible Top1cc configuration to preserve the integrity of the rDNA.

INTRODUCTION

The DNA of a cell is constantly participating in molecular transactions associated with gene transcription, DNA replication and repair. During S-phase, all these processes operate in parallel; RNA polymerases share their template with DNA polymerases moving along chromosomes and DNA repair proteins fixing DNA damage. Not only does this generate opportunities for collisions between the transcription and replication machineries, but also local DNA topological stress that requires constant release by specialized DNA topoisomerases. Topoisomerase malfunction therefore leads to an accumulation of aberrant DNA structures and, thereby, threatens genome integrity.

DNA replication encounters various obstacles such as DNA lesions or DNA-bound proteins that may impede or block replication fork (RF) progression. At programmed replication fork barriers (RFB), replication-blocking proteins bind to specific DNA sequences. In *Escherichia coli*, binding of the Tus protein to a terminator DNA sequence ensures replication termination in a defined region (1). Apart from replication termination, programmed RFBs may also function to prevent collisions between replication and transcription machineries, a potential cause of genome instability. The eukaryotic ribosomal DNA (rDNA) is particularly interesting in this respect, given that rRNA genes are continuously transcribed at high levels, irrespective whether the rDNA happens to be simultaneously replicated. The rDNA generally consists of numerous repeat units organized in tandem arrays within the nucleolus. Each rDNA unit harbours an RFB at the 3′-end of a highly transcribed rRNA gene, a feature that is highly conserved among eukaryotes [reviewed in (2)].

In budding yeast, the rDNA consists of a single array of 150–200 identical repeats on chromosome (Chr) XII, each comprising the transcriptional units *35S* and *5S*, an origin of replication (ARS) and a unidirectional ribosomal RFB (rRFB). A core rRFB sequence of ~100 bp is sufficient to recruit and bind sequence-specifically Fob1, a protein essential for the RF-blocking activity of the rRFB (3,4). The rRFB consists of one major (RFB1) and two minor (RFB2, RFB3) blocking sites that arrest altogether ≥90%

*To whom correspondence should be addressed. Tel: +41 616 953 060; Fax: +41 612 673 566; Email: olivier.fritsch@unibas.ch
Correspondence may also be addressed to Primo Schär. Tel: +41 61267 0767; Fax: +41 61267 3566; Email: primo.schaer@unibas.ch
Present address:
Vincent Dion, Center for Integrative Genomics, Faculty of Biology and Medicine, University of Lausanne, 1015 Lausanne, Switzerland.

© The Author(s) 2014. Published by Oxford University Press.
This is an Open Access article distributed under the terms of the Creative Commons Attribution Non-Commercial License (http://creativecommons.org/licenses/by-nc/3.0/), which permits non-commercial re-use, distribution, and reproduction in any medium, provided the original work is properly cited. For commercial re-use, please contact journals.permissions@oup.com

Downloaded from https://academic.oup.com/nar/article-abstract/42/8/4985/1073375/Reversible-Top1-cleavage-complexes-are-stabilized
by WWZ Bibliothek (Oeffentliche Bibliotherk der UniversitÃ¤t Basel) user
on 10 October 2017

of encountering RFs (5–7) without eliciting a checkpoint response (3) and force them to progress codirectionally with transcription through the highly transcribed *35S* gene (8). Due to its repetitive structure, the rDNA is prone to non-conservative recombination that can generate gains or losses of repeat units (9). While such events are crucial to restore the wild-type repeat number after accidental rDNA expansion or contraction, recombination between homologous rDNA repeats needs to be tightly regulated to prevent rDNA instability. Fob1 plays a major but ambivalent role in this context, having pro- and anti-recombinogenic properties (10). Consistently, Fob1-dependent DNA double-strand breaks (DSBs) were observed at the rRFB (9,11–13), but their molecular nature has remained elusive, and we showed previously that these DSBs are not substrate for canonical DSB repair (14).

A number of studies suggest a complex structural organisation of the rDNA, including the anchoring of the repeats to the nuclear membrane (15–17). This anchoring, mediated through the rRFB, involves Fob1 association with Tof2 and the cohibin complex, which in turn interacts with proteins of the inner nuclear membrane (15–17). Disruption of this association by deleting cohibin or one of the inner nuclear membrane proteins Heh1 or Nur1 destabilizes the rDNA repeat structure, suggesting that perinuclear attachment is crucial for the integrity of the locus (15,16). However, such anchorage is likely to impose mobility constraints to the rDNA, thereby increasing the topological stress created by replication and transcription and, hence, creating a need for continuous relaxation. Accordingly, DNA topoisomerases are specifically required for rDNA maintenance and functionality (18). In budding yeast, the conserved type IB DNA topoisomerase Top1 has been associated with the appearance of DNA nicks near the RFB (19), plays an important role in rRNA-gene transcription (18,20,21), PolII silencing (22–24) and, interestingly, in suppressing mitotic recombination in the rDNA (25–27). However, the mode of action underlying the specialized function of Top1 in the rDNA has not been addressed.

It is generally accepted that Top1 senses DNA-topological stress by direct recognition of the torque in the DNA (28). The protein then incises one DNA strand through a reversible transesterification involving a 3′-phosphodiester-tyrosyl bond, thereby engaging in a transient Top1 cleavage complex (Top1cc) intermediate with the 3′-end of the nick. Following relaxation of the DNA helix by rotation of the unbound end, Top1 reseals the nick through the reverse transesterification reaction (29). Top1ccs can be stabilized or even converted to irreversible intermediates under the influence of topoisomerase inhibitors like camptothecin (CPT), or in the presence of DNA lesions preventing the re-ligation of the single-stranded ends (29). Exactly how the cleavage and re-ligation reactions of topoisomerases are coordinated under physiological conditions is poorly understood, but the notion is that cleavage complexes are very short-lived as their resolution is triggered immediately following relaxation of the DNA helix. Here we sought to characterize the function of Top1 at the rRFB and found that Top1ccs accumulate at the rRFB, independently of its RF-stalling activity. A 450-bp rRFB sequence is sufficient to trigger Top1cc formation independently of the rDNA context and the enrichment of Top1ccs at such sites, mediated by Fob1 and Tof2, reflects a stabilization of reversible cleavage complexes. The formation of these targeted Top1cc complexes explains the previously reported occurrence of DSBs at the rRFB in wild-type cells and implicates a physiologically regulated mode of Top1 action.

MATERIALS AND METHODS

Yeast strains and plasmids

Yeast strains are listed in Supplementary Table S1. All strains are isogenic derivatives of the closely related FF18733, FF18734 and FF18984 congenic series in an A364 background. Strains carrying eRFBs on Chr IV were constructed by PCR-mediated gene targeting using plasmids harbouring a 450-bp rRFB sequence insert. Gene deletions and tagging were achieved by standard methods. Strains with a LacO array tagged eRFB locus were constructed as described (30). For strains usage and plasmids construction see Supplementary Materials.

Chromatin immunoprecipitation with or without crosslink

For chromatin immunoprecipitation (ChIP) with crosslink, whole-cell extracts were prepared from formaldehyde-fixed cell cultures as described (31,32) with modifications (Supplementary Materials). For Top1cc immunoprecipitation (IP), non-crosslinked samples were processed as described previously (33), with some modifications. Shortly, 100 ml of an exponentially growing culture was washed once with cold 20 mM Tris–HCl pH 8.0, twice with cold FA buffer (50 mM Hepes–KOH, 150 mM NaCl, 1 mM EDTA, 1% Triton-X, 0.1% Na-deoxycholate, 0.1% SDS, 1 mM PMSF) and the cell pellet was frozen at −80°C. Cold FA (1 ml) was added to the pellet prior to cell disruption in a Fastprep-24 (MP) bead-beater (twice 40 sec at 6.5 m/s) with 0.5 mm Zirconia/silica beads. Beads were discarded and 1 ml of FA buffer was added before centrifugation for 20 min at 17 000 g, 4°C. The pellet was re-suspended in 800 µl FA buffer and kept rolling (30 min, 4°C) before sonication to an average size of 400 bp (Bioruptor, Diagenode). After adding 800 µl of FA buffer, samples were centrifuged (30 min, 10 000 g, 4°C). The supernatant was stored at −80°C and an aliquot saved as Input. IP was performed with 500 µl of supernatant (2 h, 4°C) with Dynabeads (Dynal, Life Technologies) precoated with mouse anti-Myc (9E10) antibody. Beads were then washed twice for 10 s and once for 10 min with 500 µl of modified FA buffer with 500 mM NaCl (shaking, 1400 rpm). After successive washes (shaking, 1400 rpm) with 500 µl of 10 mM Tris–HCl pH 8.0, 0.25 M LiCl, 1 mM EDTA, 0.5% NP-40, 0.5% Na-deoxycholate and 500 µl of TE pH 8.0, DNA was eluted from the beads (20 min, 65°C). IP and Input DNA were treated with 1 mg/mL Pronase (Roche) in 25 mM Tris–HCl pH 7.5, 5 mM EDTA, 0.5% NP-40, 0.5% Na-deoxycholate for 1 h at 37°C. DNA was then recovered by phenol–chloroform and isopropanol precipitation.

Downloaded from https://academic.oup.com/nar/article-abstract/42/8/4985/1073375/Reversible-Top1-cleavage-complexes-are-stabilized
by WWZ Bibliothek (Oeffentliche Bibliotherk der UniversitÃ¤t Basel) user
on 10 October 2017

DNA from ChIP of crosslinking and non-crosslinking conditions were analyzed by real-time PCR (qPCR) with SYBR-Green (QuantiTect, Qiagen) using a Rotor-Gene RG3000 system (primer sequences are available upon request) and values from IP samples were related to that of their relative Input. Samples from one ChIP experiment were run two to three times in duplicates. Mean duplicate values within each run were used for calculation.

Live-cell microscopy and image analysis

Live-cell-imaging experiments were performed using cultures of yeast cells in the appropriate SC drop out to select for the presence of the CFP-Nop1 (pFN5 and pFN6) or GFP-Nup49 (pUN100-GFP-Nup49) expressing vectors as described (34–36) Two independent cultures were imaged on different days for each genotype. A single user analyzed the images without knowledge of the genotypes. Deconvolution was achieved using the Huygens Remote Manager (37) (see Supplementary Materials for imaging and analysis details).

Cell growth and CPT treatments

Cell-cycle arrest at the end of G1 was induced in liquid YPD cultures (7.5×10^6 cells/ml) with 2 μg/ml α-factor (GenScript) for 2 h at 30°C. Cells were released from G1-arrest by the addition of 50 μg/ml Pronase. G1-arrest and release were validated by FACS.

1D- and 2D-gel electrophoresis and Southern blots

Isolation of DNA in agarose plugs was done as described (11), with some modifications (see Supplementary Materials). Gels and alkaline Southern blotting were done as described (13,14). 1D-gel conditions: 24 h, 70 V, 1% agarose without EtBr. PCR-amplified probes were radioactively labelled with (α-^{32}P)-dCTP (6000 Ci/mmol, PerkinElmer). rDNA copy number was estimated from BamHI-digested genomic DNA of late-exponential cultures isolated in agarose plugs as recommended in the Biorad's CHEF-DR manual. PFGE was performed as described (14), with the exception that the length of the run was 48 h.

Quantification of ERC formation

Genomic DNA was isolated from late logarithmic-phase cultures in YPD media using Qiagen genomic tips. Undigested DNA was loaded on 0.8% agarose gels and run in 1× TAE buffer for 17 h at 65 V without EtBr. Southern blots with rDNA probe1 and quantitation were performed as for 2D-gels. The prominent signal corresponding to the bulk of rDNA was used for normalization across genotypes.

Quantitation of DSBs and statistical methods

Quantitation of 1D- and 2D-gels was performed as described (14). See Supplementary Materials for RI definition and further details. Statistical analysis was performed with the Prism software. When not else mentioned, unpaired 2-tailed T-tests were performed for comparisons. For Figure 4A and C paired 2-tailed T-tests were performed. For Figure 5C, one-sample 2-tailed *T*-tests against a theoretical mean were applied for mutants versus wild-type comparisons.

RESULTS

Fob1-dependent Top1ccs are enriched at the rRFB

Based on the observation that Top1 controls the appearance of DNA nicks near the rRFB (19), we investigated more specifically the interaction between Top1 and the rRFB in budding yeast. We first compared Top1 and Fob1 occupancies along the rDNA unit by ChIP following crosslinking in asynchronous cultures. As observed previously (17,38), Fob1 was highly enriched at the rRFB with a mild secondary peak in the *35S* promoter region (Figure 1A). By contrast, Top1 enrichment spread all over the rDNA unit showing only a slight increase at the rRFB (Figure 1A). In a *fob1*Δ background, Top1 association with the rDNA was generally reduced, most strongly (~3-fold) at the rRFB (Figure 1A). Thus, cross-linked ChIP supported an association of Top1 with the rDNA but did not reveal any preferential sites of enrichment.

We then used ChIP under non-crosslinking conditions to localize specifically Top1ccs, i.e. Top1 molecules that are actively engaged in DNA nicking and covalently bound to the 3′-end of the DNA via their Tyr727 residue (Figure 1B) (33). With this method, we detected a strong enrichment of Top1cc at the rRFB relative to sites in the *35S* (Figure 1C and D) and a mild enrichment in the *35S* promoter region, similar to crosslinked Fob1 ChIP (Figure 1D). In the absence of Fob1, Top1cc association with the rRFB was completely lost, whereas the small enrichment in the *35S* promoter region remained unaffected (Figure 1D). From these results, we conclude that Top1cc formation occurs with different specificity and kinetics along the rDNA unit with the rRFB being a hotspot. Importantly, the different enrichment patterns of Top1cc (without crosslinking) and Top1 (with crosslinking) suggest that Top1 associates with chromatin throughout the rDNA but is preferentially engaged in nicking at the rRFB. This may reflect an increased enzymatic turnover and/or a stabilization of the Top1cc intermediate specifically at the rRFB.

Top1cc is detected at ectopic rRFBs outside the rDNA context

To gain further insight into the nature and context-dependency of Top1cc at the rRFB, we established a novel, strategically designed ectopic rRFB (eRFB) model. We introduced a 450-bp sequence containing the rRFB region near an early firing origin of replication (ARS453) on Chr IV (Figure 2A). As this region lacks detectable replication-origin firing within 50 kb on the distal side of the resulting eRFB (eRFB1) (39), Fob1 binding to eRFB1 should pause RFs originating from ARS453 before they encounter a converging fork. The introduced eRFB sequence was indeed sufficient to recruit Fob1 (Supplementary Figure S1) and assemble a functional RF-pausing site (Figure 2B), as observed previously at a different locus (3). To distinguish Fob1-

Downloaded from https://academic.oup.com/nar/article-abstract/42/8/4985/1073375/Reversible-Top1-cleavage-complexes-are-stabilized
by WWZ Bibliothek (Oeffentliche Bibliotherk der UniversitÃ¤t Basel) user
on 10 October 2017

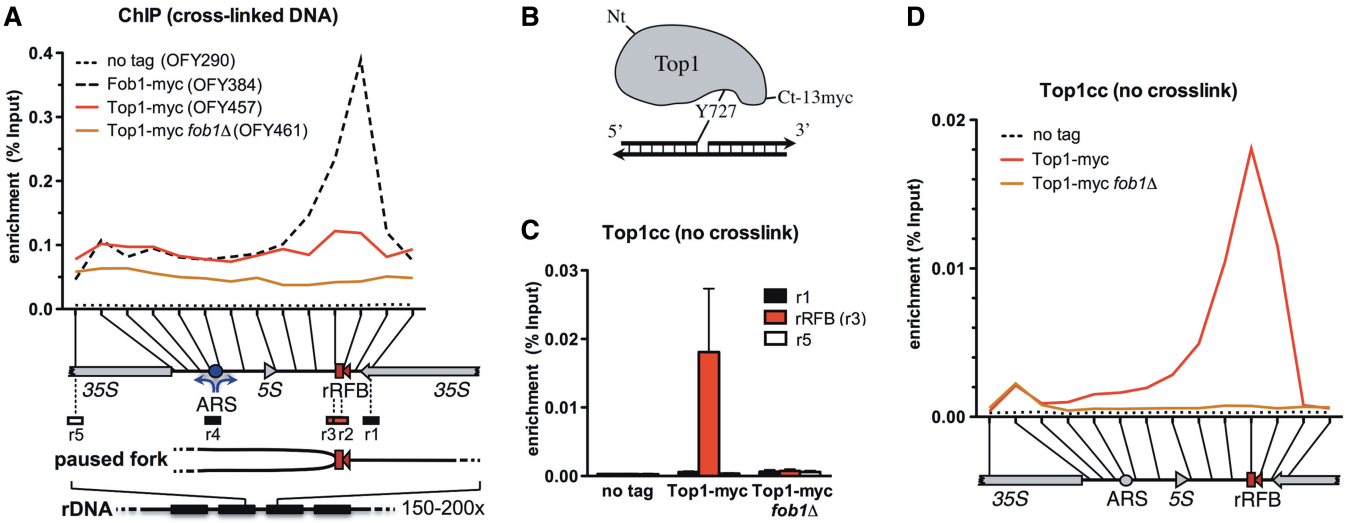

Figure 1. Top1ccs accumulate at the rRFB. (**A**) Mapping of Top1 in the rDNA by standard ChIP. Exponentially growing cells were crosslinked with formaldehyde before ChIP. Shown is the mean enrichment ($N = 3$). The position of qPCR primer sets is indicated on one rDNA unit, together with those used in (**C**) and (**D**) with the unidirectional rRFB blocking RFs as depicted. *35S* and *5S*, rRNA transcription units. (**B**) Schematic representation of myc-tagged Top1cc. While nicking one strand, Tyr727 engages transiently but covalently with the 3′-phosphodiester at the nick. (C) Top1cc is enriched at the rRFB. Top1cc ChIP was conducted from non-crosslinked exponentially growing cells of yeast strains as in (A). The mean ($N = 4$) with SEM is shown. Primer-sets location, see (A). (D) Mapping of Top1cc along the rDNA unit by non-crosslinked ChIP as in (C). The mean ($N = 4$) is shown. qPCR primer set positions are indicated. Strains as in (A).

mediated from stalling-triggered effects, we introduced a second eRFB (eRFB2) 6-kb apart from the first, in either the same (direct repeat) or the opposite (indirect repeat) orientation relative to eRFB1 (Figure 2A). The eRFB2 in the same orientation as eRFB1 will pause progression of forks emanating from ARS453 (and leaking from eRFB1), whereas the eRFR2 in the opposite orientation will be permissive and, thus, not accumulate pausing forks. Although Fob1 was enriched at the eRFB2 in either orientation (Supplementary Figure S1), paused RFs only accumulated in the direct-repeat configuration (Figure 2C), confirming that no or only very few RFs were approaching from the ARS453-distal side (39). The eRFB2 constructs thus allow the assessment of RF stalling-independent functions of Fob1.

To confirm that the eRFB is outside of the rDNA context and not anchored to the nuclear membrane despite the insertion of rDNA sequence—this was not addressed for previously published eRFB strains (3)—we assessed the position of the eRFB in the nucleus by fluorescence microscopy. We inserted ~250 lacO repeats near the eRFB1, allowing for the measurement of its relative distance to the nucleolar periphery upon ectopic expression of YFP-LacI, visualizing the location of the lacO array and of CFP-Nop1 fusions marking the nucleolus (Figure 2A). In the wild-type, but also in *fob1*Δ and *top1*Δ backgrounds, the eRFB1 sub-nuclear localization was clearly extranucleolar, irrespective of the cell-cycle stage and deletion of eRFB1 confirmed that its ectopic insertion did not alter the authentic localisation of this Chr IV locus relative to the nucleolus (Figure 2D). In contrast, a wild-type strain carrying a TetO array in the rDNA and an integrated TetI-mRFP1, highlighting an internal rDNA locus (40) produced fluorescence signals clearly located in the nucleolus. We then assessed the position of the eRFB1 locus relative to the nuclear periphery as visualized by a GFP–Nup49 fusion marking the nuclear periphery. The eRFB1 locus was not associated with the periphery irrespective of the presence or absence of the barrier (Figure 2E), indicating that eRFB1 is not sufficient to mediate perinuclear anchoring. These results show that the eRFB insertion preserves the authentic location of the locus with respect to the nucleolus and the nuclear periphery making it a suitable model to analyze rRFB functions outside the complex organisation of the rDNA. Using this eRFB system, we detected Fob1-dependent peaks of Top1cc enrichment at the eRFB1 and eRFB2 (Figure 3B and C), similar to the situation at the rRFB in the rDNA (Figure 1D). Given the spatial separation of the eRFB from the nucleolus, these results suggest that Top1cc at the rRFB in wild-type cells is formed independently of the rDNA context and that the 450-bp rRFB sequence is sufficient to trigger Top1cc formation outside the rDNA.

Top1cc associates strand-specifically with the eRFB independently of RF-stalling

Investigating the link between RF-pausing and Top1cc formation at the rRFB, we found the levels of Top1cc enrichment at the rRFB to be similar in G1- and S-phase of the cell cycle (Figure 3B). This was true both at ectopic and ribosomal sites, establishing that Top1cc formation at the rRFB is not restricted to S-phase. To exclude that RF pausing induces nicks that persist throughout the cell cycle, we mapped Top1cc along the eRFB1/eRFB2 locus in the direct- and indirect-repeat configuration (Figure 3C). Top1cc was strongly enriched at both eRFBs, independent of their orientation,

Downloaded from https://academic.oup.com/nar/article-abstract/42/8/4985/1073375/Reversible-Top1-cleavage-complexes-are-stabilized
by WWZ Bibliothek (Oeffentliche Bibliotherk der UniversitÃ¤t Basel) user
on 10 October 2017

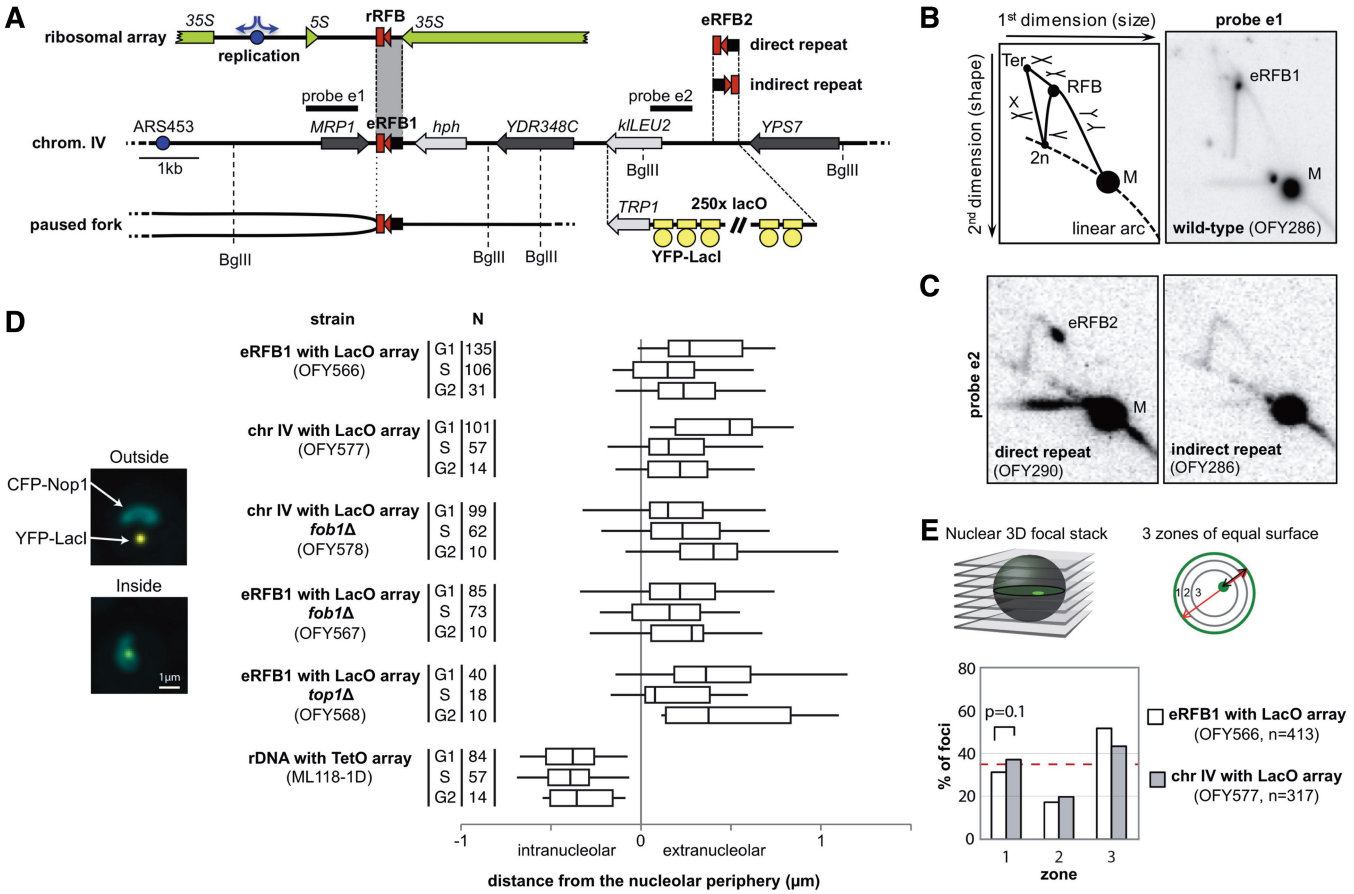

Figure 2. A 450-bp rRFB sequence is sufficient to trigger a Top1cc signal outside the rDNA. (**A**) The eRFB model on Chr IV. One rDNA unit is shown as reference. The 450-bp rRFB sequence (grey) used as eRFB was inserted at two ectopic sites (eRFB1 and eRFB2) near the early firing origin ARS453. For live-cell microscopy, an array of 250 LacO repeats was inserted instead of eRFB2. (**B**) The eRFB1 is proficient for RF stalling. Scheme and Southern blot of DNA species obtained after 2D-gel electrophoresis of BglII-digested genomic DNA from exponential cultures of a wild-type strain carrying the eRFB1. Probe e1, see (A) M, monomer; RFB, rRFB-stalled RFs; Ter, converging RFs; 2*n*, molecules of twice the monomer size. Note that faint spots on the left of the M and eRFB1 signals correspond to incomplete digestion of the BglII site between *PAL1* and *hph*. (**C**) Fork-pausing activity at the eRFB2. Southern blots of 2D-gels as in (B) except for probe e2 (A). (**D**) The eRFB1 locus is not recruited to the nucleolus. eRFB1 strains harbour a LacO array with an integrated YFP-LacI gene (A) and a CFP-Nop1 expression plasmid for nucleolar staining. To assess the localization of the ectopic locus without a barrier, eRFB1 was exchanged for a *natNT2* cassette. (Left) Representative images for eRFB1 localization relative to the nucleolus. Shown are examples of strain OFY566 with extra- and intranucleolar localization, respectively. (Right) Quantification of nucleolar localization. The distance distribution between the tagged genomic locus and the nucleolar periphery, as obtained from the CFP-Nop1 signal, is plotted as a box plot (boxes, 25th–75th percentiles; whiskers, 5th and 95th percentiles; vertical bars, medians). (E) A single eRFB is not sufficient to anchor a locus to the nuclear periphery. (Top) Optical slices were taken in cells expressing GFP–NUP49 fusion that demarcates the nuclear periphery. Three zones of equal surface were defined for distance measurements (35). A locus that is randomly distributed throughout the nucleus is expected to have an equal chance of being in any one zone. (Bottom) Location of the eRFB1 locus on Chr IV in the presence or absence of the barrier. Dashed red line, expected random distribution. *P*-value is for a $\chi 2$ test with df = 1 for zone 1 between the two strains.

indicating that Top1cc accumulates at the eRFB2 even in the absence of RF-pausing at this site. In line with this, deletion of *TOF1*, encoding a factor required for RF stalling at an RFB (Figure 3D) (3), did not significantly affect Top1cc enrichment at eRFB1 and eRFB2 (Figure 3E). Further, to exclude genomic context effects, we also inverted the eRFB1 and analyzed resulting strains now carrying two non-blocking eRFBs (Figure 3D and E). Top1 was indeed associated with the non-blocking eRFB1, corroborating that Top1cc at the eRFB forms independently of RF stalling. Since Top1cc accumulation requires Fob1 but not RF pausing (Figures 1D and 3C), these findings strongly suggest that Fob1 recruits and/or stabilizes Top1cc at the eRFB independently of DNA replication. Importantly, Top1cc enrichment was asymmetric with respect to the 450-bp eRFB insertion. While Top1cc was enriched next to the side that is capable of RF stalling, it was absent from the opposite side of the insertion (Figure 3C and E; compare primer sets 2/3 for eRFB1 and 5/6 for eRFB2). This is best explained by a preferential breakage of Top1 nicked sites during DNA sonication and a subsequent enrichment of DNA fragments with the 3′-attached Top1cc by Top1–ChIP. However, the data do not exclude the possibility that the asymmetry of Top1cc enrichment over the 450-bp eRFB sequence (Figure 3F) is caused by the unequal distance of the PCR probes to the

Downloaded from https://academic.oup.com/nar/article-abstract/42/8/4985/1073375/Reversible-Top1-cleavage-complexes-are-stabilized
by WWZ Bibliothek (Oeffentliche Bibliotherk der UniversitÃ¤t Basel) user
on 10 October 2017

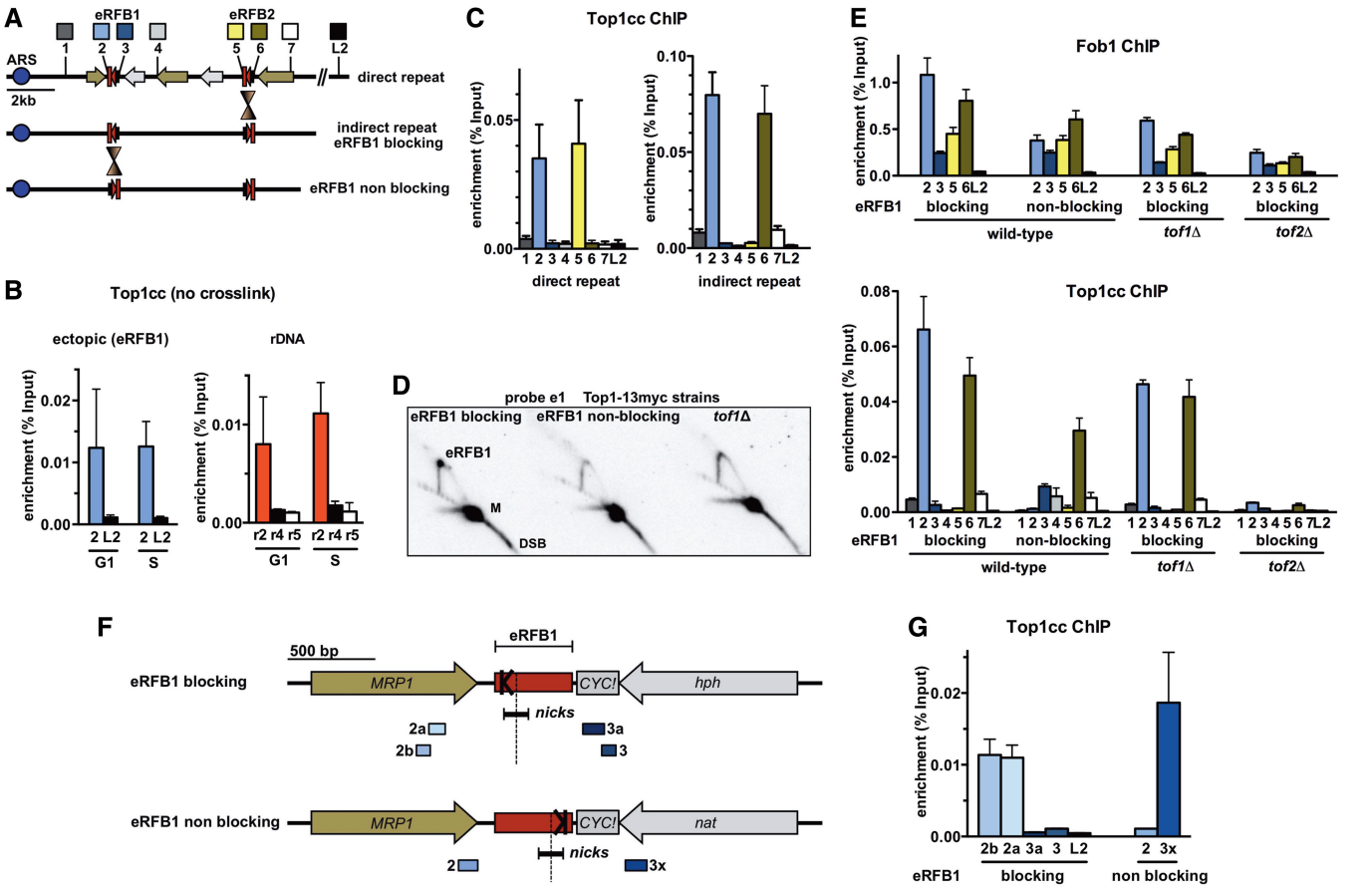

Figure 3. Top1cc enrichment at an eRFB is strand-specific and independent of RF stalling. (**A**) Orientation of eRFBs and localization of qPCR primer sets in eRFB strains. The control L2 set is located in a late replicated region of Chr IV. (**B**) Top1cc is enriched at the rRFB and eRFB1 in both G1- and S-phases. Wild-type cells expressing Top1–myc (OFY457) were arrested in G1 and released into S-phase for 30 min prior to non-crosslinked ChIP. The mean enrichment ($N = 2$) is shown with SD. Primer-sets location, see (A) and Figure 1A. (**C**) Asymmetry of the Top1cc signal at eRFB1 and eRFB2. Top1cc ChIP with primer sets as indicated in (A). The mean with SEM is shown ($N = 3$). (**D**) RF-stalling activity at the eRFB1 of *tof1Δ* and eRFB1 blocking and non-blocking strains. Southern blot of a 2D-gel from exponentially growing cells as in Figure 2B. (**E**) Requirements for Top1cc accumulation at eRFBs. Mean enrichments from ChIP experiments for Fob1-myc (crosslink, $N = 4$) and Top1cc (no crosslink, $N = 3$) are shown. Primer sets for qPCR, see (A). (**F** and **G**) The Top1cc signal at the eRFB1 is strand-specific. (F) Scheme of the eRFB1 region in the blocking versus non-blocking orientation (as referred to ARS453). Black symbols |< and >| indicate the main RF pausing site (RFB1) with blocking RFs coming from the left or right, respectively. For each eRFB1 orientation, qPCR probes at equidistant sites from the centre of Top1 induced nicks are indicated (black line). (G) Mean enrichment values ($N = 3$, SEM) for non-crosslinked Top1cc ChIPs with strains and primers as depicted in (F).

area where Top1 nicks are located. We addressed this by qPCR of Top1cc ChIP experiments using pairs of primer-sets equidistant to the Top1 nicks (Figure 3F). The detection of a strong Top1cc signal on the blocking side and no signal on the non-blocking side in each of the eRFB1 orientation, allowed us to exclude this hypothesis (Figure 3G). This given, the asymmetric enrichment is strongly indicative for Top1 being positioned to the rRFB to specifically incise the DNA strand corresponding to the parental lagging strand ahead of a potential rRFB-paused RF, consistent with results from the mapping of Top1 controlled nicks (19,41).

Top1 accumulation at the rRFB reflects stabilization of a transient cleavage complex

The enrichment of Top1ccs at both ribosomal and ectopic RFBs might reflect an accumulation of irreversibly bound Top1ccs. Processing of irreversible Top1ccs involves both proteolytic degradation of Top1 and cleavage of the DNA 3′-end that is covalently attached to Tyr727. The enzyme dedicated to Top1cc processing is Tdp1, but other factors provide complementary activities and can even substitute for Tdp1, most prominently the Rad1 and Mus81 nucleases (42,43). Given the poor growth and pleiotropic phenotype of the triple *tdp1Δ rad1Δ mus81Δ* mutant, we resorted to monitor the potential accumulation of irreversible Top1cc in *tdp1Δ rad1Δ* and *tdp1Δ mus81Δ* double mutants, where defects in Top1cc repair are detectable (43). We generated these strains, confirmed their sensitivity to CPT (Supplementary Figure S2) and assessed Top1cc enrichment at eRFB1 by non-crosslinked ChIP (Figure 4A). We found no significant change in Top1cc levels in these double mutant strains compared to the wild type. To rule out that Top1cc enrichment at the eRFB is saturated in the wild type, we added CPT to permeabilized cells prior to ChIP; permeabilization allowing for a rapid

Downloaded from https://academic.oup.com/nar/article-abstract/42/8/4985/1073375/Reversible-Top1-cleavage-complexes-are-stabilized
by WWZ Bibliothek (Oeffentliche Bibliotherk der UniversitÃ¤t Basel) user
on 10 October 2017

and efficient CPT uptake. Under these conditions, Top1cc levels were clearly increased (Supplementary Figure S3), suggesting that potential effects of Top1cc repair defects at the eRFB could be detected. The unchanged level of Top1cc in *tdp1*Δ *rad1*Δ and *tdp1*Δ *mus81*Δ strains thus indicates that Top1ccs formed at the eRFB are not subject to repair but remain reversible with the nicked configuration stabilized but prone for re-ligation. We therefore conclude that stabilized Top1ccs at the rRFB are physiological intermediates.

Tof2 mediates Top1cc accumulation at eRFBs and stabilizes Fob1

The Fob1 dependency of Top1cc formation at the rRFB raises the possibility that Fob1 positioning also requires Top1, and that the two proteins engage in a Top1cc-stabilizing functional interaction. To assess the existence of such a complex, we performed Fob1 ChIP from *TOP1* wild-type and deleted strains. Because of the repetitive structure and the nuclear context of the endogenous rRFB, we focused on the eRFB. Fob1 enrichment at the eRFB was indeed reduced in *top1*Δ cells as compared to wild-type cells (Figure 4B and Supplementary Figure S4), suggesting that Top1 stabilizes the Fob1-eRFB interaction and, consequently, that the two proteins are part of a functional complex. Fob1 seems to be the central organizer of this complex as it is a prerequisite for Top1cc association with the eRFB but remains detectable in the absence of Top1. Searching for additional components of the complex, we considered Tof2. Tof2 physically interacts with both Fob1 and Top1 (17,44) and is therefore implicated as a mediator of an rRFB-associated function of Top1. We assessed the influence of *TOF2* deletion on Top1cc and Fob1 association with the eRFBs. Fob1 enrichment at eRFB1 and eRFB2 in *tof2*Δ cells was reduced to less than half of that in wild-type cells, whereas Top1cc enrichment was almost completely lost (~5% of the wild-type level, Figure 3E). Thus both Fob1 and Top1cc enrichment at the eRFBs is modulated by Tof2, suggesting that the three proteins are part of an rRFB binding protein complex that mediates targeted and strand-specific Top1 activity.

DSBs detected at ectopic and endogenous rRFBs depend on Top1 activity

RFs paused at the rRFB have been proposed to break under physiological conditions (9,11–13), based on the detection of DNA-replication associated DSB signals in 1D and 2D-gel experiments. As these apparent DSBs did not appear to be substrate for the canonical DSB-repair systems (14), we wondered whether they might originate from Top1-induced nicks at the rRFB (Figure 5A), as the DNA duplex between the nick and the arrested RF might melt during DNA isolation (orange fragment on Figure 5A). We performed 2D-gels using DNA isolated from asynchronous cell cultures (Figure 5B), quantified the DSB signal and normalized it to replication intermediates (RIs) (14). In *top1*Δ cells, the level of broken RFs at the rRFB decreased to 35% of that in wild-type cells ($P = 0.032$; Figure 5C). We also detected a DSB signal

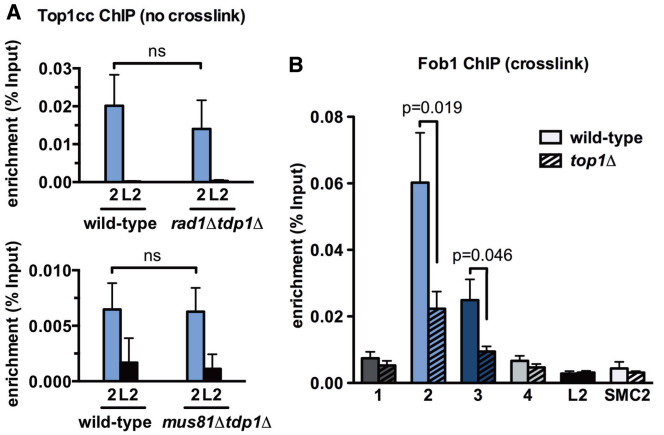

Figure 4. Stabilization of Top1cc at the eRFB1. (**A**) Contribution of irreversible-Top1cc repair pathways to Top1cc enrichment at the eRFB1. Top1cc ChIP from exponentially growing cells. Matching wild-type/mutant pairs were isolated by crosses. Location of qPCR primer sets, see Figure 3A. (**B**) Fob1 enrichment at the eRFB1 is partially dependent on Top1. Mean values from five cross-linked ChIP experiments are shown for one representative wild-type/*top1*Δ strains pair. SMC2, qPCR primer set in the *SMC2* gene. Location of other primer sets, see Figure 3A.

at the eRFB1 in wild-type cells (Figure 3A and Supplementary Figure S5A); as in the rDNA, the DSB signal was absent in *fob1*Δ cells (Supplementary Figure S5A) and reduced in *top1*Δ cells (Supplementary Figure S5B). Thus, most of the DNA breaks at these RFBs arise in a Top1-dependent manner. To further differentiate between an enzymatic and a structural contribution of Top1, we tested the effect of CPT treatment on the DSB signal. As CPT stabilizes Top1cc, it should increase the steady-state level of Top1-dependent nicks at the rRFB (19). We exposed permeabilized spheroplasts to CPT prior to 1D-gel analysis (Supplementary Figure S6). Whereas the level of broken RFs at the rRFB increased 1.8-fold upon CPT treatment in wild-type cells, it remained unaltered in *top1*Δ cells, showing that Top1ccs and, thus, the catalytic activity of Top1 are responsible for the appearance of the DSB signal at the rRFB.

DSBs induced at the rRFB upon *SGS1* disruption occur independently of Top1

In the absence of the RecQ helicase Sgs1, the level of broken RFs at the rRFB increases on 1D- and 2D-gels (12,14). We reasoned that, in contrast to the breaks in wild-type cells, these additional breaks result from insufficient stabilization of the rRFB-paused RF and, thus, may be of a different molecular nature. As Top1cc accounted for most of the DSB signal on 2D-gels in wild-type cells (Figure 5C), we asked whether the additional breaks observed in *sgs1*Δ cells are also Top1-dependent. We measured DSBs at the endogenous rRFB that exhibits a better dynamic range for DSB quantitation than the eRFB. Disruption of *SGS1* led to a moderate but significant increase of DNA breaks at the rRFB both in the wild-type (1.3-fold) and *top1*Δ (2.3-fold) backgrounds (Figure 5C). Thus, Top1-independent breaks accumulate

Downloaded from https://academic.oup.com/nar/article-abstract/42/8/4985/1073375/Reversible-Top1-cleavage-complexes-are-stabilized
by WWZ Bibliothek (Oeffentliche Bibliotherk der UniversitÃ¤t Basel) user
on 10 October 2017

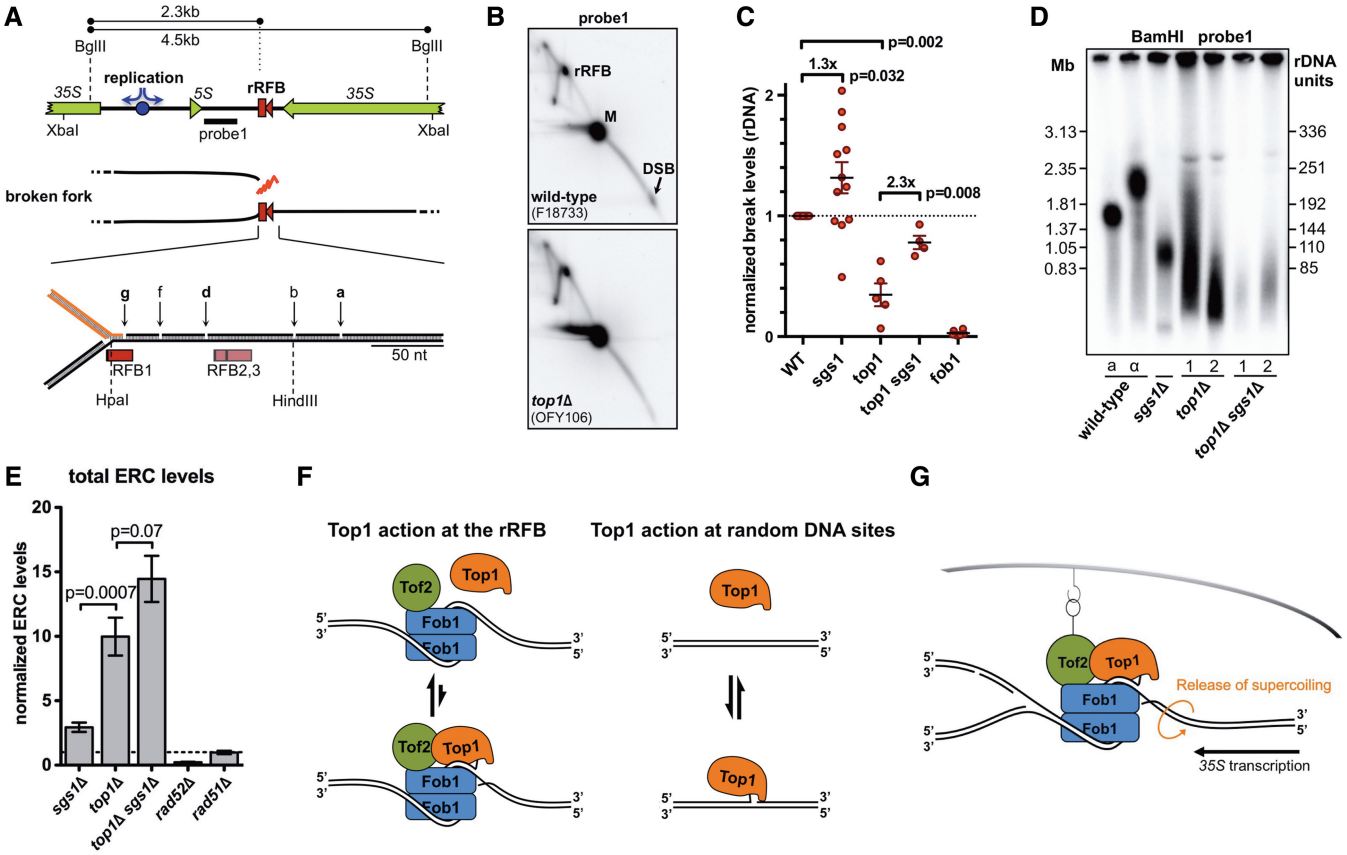

Figure 5. Function of Top1cc at the rRFB and link with previously reported DSBs. (**A**) Map of one rDNA unit and close-up on the DNA nicks (*a*, *b*, *d*, *f* and g) observed at the rRFB on the upper strand (13), *a* and *d* showing Top1 dependency (41). (**B**) Top1 contributes to the DSB signal on 2D-gels. Representative Southern blots of 2D-gels from exponential cultures. M, monomer; rRFB, rRFB-stalled RFs; DSB, broken RFs. (**C**) Quantification of DSB levels from experiments as in (B). Dots represent DSB levels relative to RIs (see Materials and methods section) and normalized to DSB levels from wild-type DNA on the same gel. Means ± SEM are indicated. (**D**) Impact of Top1 on rDNA copy-number maintenance. Southern blot of genomic DNA digested with BamHI, which does not cut within the rDNA, analysed by PFGE. (**E**) ERC formation. Undigested genomic DNA from young cells was separated on agarose gels, which were subjected to Southern blot analysis using rDNA probe1 (Figure 5A). All ERC signals, see (13) for details, were quantitated from at least three experiments in duplicate, corrected for rDNA loading and normalized to wild-type. The mean ± SEM is plotted. (**F** and **G**) A model for Top1cc formation and function at the rRFB. See text for details. (F) Top1ccs are preferentially stabilized at the rRFB as compared to genome-wide occurring Top1ccs. (G) Top1ccs stabilize the rDNA by relieving torsional stress deriving from the perinuclear anchoring of the rRFBs.

in the absence of Sgs1; probably reflecting collapsed RFs that are prone to recombination.

Reduced rDNA stability in the absence of Top1

We showed that Top1 nicks are stabilized at the rRFB, providing a mechanism for the continuous release of torsional stress. Assuming that stabilized nicks prevent unscheduled and possibly recombinogenic breaks, rDNA recombination should increase upon *TOP1* deletion. Increased rDNA recombination in *top1*Δ cells is supported by the reduced and variable rDNA copy number (Figure 5D) as well as an increased failure of Chr XII of exponentially growing cells to enter the gel (45) in pulse-field gel electrophoresis (PFGE). rDNA recombination also gives rise to elevated excision of extrachromosomal ribosomal circles (ERCs). Indeed, ERC levels are increased in *top1*Δ cells (Figure 5E) (27), suggesting that Top1-dependent nicks contribute to the preservation of DNA integrity. Similar to *top1*Δ cells, *sgs1*Δ cells possess an unstable rDNA copy number (Figure 5D) (46) and an increased level of ERCs (Figure 5E) (47). Normalized Top1cc levels at the rRFB, however, remain essentially unaltered upon *SGS1* disruption (Supplementary Figure S7), whether at the eRFB1 or the authentic rRFB in the rDNA, suggesting that Top1ccs at the rRFB do not contribute to the rDNA instability of *sgs1*Δ cells. PFGE of DNA from *top1*Δ *sgs1*Δ cells did not reveal any further instability than that seen in either single mutant (Figure 5D). Thus, both Top1 and Sgs1 function in rDNA homeostasis. While positioned DNA incision by Top1 at the rRFB promotes rDNA stability, DSBs generated in *sgs1*Δ cells cause instability.

DISCUSSION

Top1 releases DNA torsional stress generated by DNA replication, transcription or repair by nicking and religating DNA single strands. This involves the formation of Top1ccs, transient covalent intermediates linking Top1

Downloaded from https://academic.oup.com/nar/article-abstract/42/8/4985/1073375/Reversible-Top1-cleavage-complexes-are-stabilized
by WWZ Bibliothek (Oeffentliche Bibliotherk der UniversitÃ¤t Basel) user
on 10 October 2017

with the DNA. We show that Top1ccs are strongly enriched at the yeast rRFB, a site where DNA nicks were previously correlated with Top1 activity, in the absence of topoisomerase poisons, suggesting that persistent Top1-mediated strand cleavage is targeted to the rRFB under physiological conditions. Whereas ChIP without prior chemical crosslinking yielded a strong peak of Top1cc enrichment at the rRFB, crosslinking resulted in only little specific Top1 enrichment at this site (Figure 1). Thus, although Top1 associates with the rDNA repeat along its entire length, the steady-state level of cleavage complexes is specifically increased at the rRFB. Given that these Top1ccs are not subject to topoisomerase repair by the canonical pathways (Figure 4A) and that the loss of Top1 destabilizes the rDNA structure (Figure 5D and E), the data suggest that Top1 is targeted to the rRFB where it accumulates in reversible cleavage complexes in a physiological process of rDNA maintenance. Although we cannot strictly rule out the possibility that the enrichment of Top1cc at the RFB reflects an increased turn-over of Top1 cleavage cycles, the data favour a model in which the normally transient Top1cc intermediates are stabilized at the RFB. Both scenarios support that Top1ccs, and hence the DNA nicks, are subject to physiological regulation in the context of genome maintenance.

The stabilization of Top1cc would implicate some form of regulation of the re-ligation step of the of Top1 reaction. This may provide a mechanism for controlled release of the DNA torsional stress building up in the rDNA due to transcription and replication activities and aggravated by the mobility constraints imposed by the perinuclear anchoring of the rDNA repeats (15–17). The purpose of such strategic positioning of persistent but reversible Top1 nicks at the RFB would thus be to continuously normalize DNA topology and, thereby, increase the stability of this special genomic region. Consistently, recombination in the rDNA increased upon *TOP1* deletion, as we observe an unstable and decreased rDNA length associated with increased formation of ERCs, an rDNA recombination product (Figure 5D and E) (25). This phenotype caused by the absence of Top1 could be well explained by a build-up of torsional stress in the rDNA, which is then compensated for by the random induction of unscheduled DNA breaks, by Top2 or Top3 for example. Such unscheduled breaks could occasionally trigger recombination and finally the formation of ERCs.

Top1 does not only prevent unscheduled recombination in the rDNA, it also stabilizes the Fob1 complex as implicated by a reduced Fob1 ChIP signal upon *TOP1* deletion (Figure 4B). Gains or losses in rDNA copy number are quickly normalized by unequal sister-chromatid exchange in wild type but not in *fob1*Δ yeast cells, in which also ERC formation is abolished (48,49). While *TOP1* deletion results in an unstable rDNA repeat number, *FOB1* deletion completely abolishes copy number changes (10). The different effects of *TOP1* and *FOB1* deletion on rDNA recombination are consistent with Fob1 being the main regulator of the rRFB complex. In the absence of Fob1, neither RF stalling nor perinuclear anchoring will occur. In this situation, less torsional stress is created, lowering the need for Top1-dependent release of DNA torsion. Thus, both Top1 and Fob1 are important for rDNA stability, but they impact at different levels of a common underlying pathway.

Using ectopically integrated rRFBs (eRFB1 and eRFB2), we show that Top1cc accumulation at the rRFB requires neither the authentic nucleolar rDNA context nor the perinuclear anchoring. Thus, the 450-bp rRFB-containing sequence carries sufficient information to mediate Top1cc accumulation. The eRFBs on Chr IV reside in a genomic context with low transcriptional activity as opposed to the situation on the rRFB. The presence of Top1 nicks at eRFB1 thus suggests that Top1cc enrichment is independent of the proximity to the highly transcribed *35S*. Moreover, the comparable enrichment of Top1cc at eRFB1 and eRFB2 as well as in strains with inverted orientations of the eRFBs indicates that Top1cc levels are not influenced by the local transcriptional activity (Figure 3). This is in accordance with previous work showing that the occurrence of CPT-inducible nicks at the rRFB is not affected by altering the transcription efficiency of RNA PolI (19).

Remarkably, we show that the formation of Top1ccs at the rRFB is restricted to the DNA strand defined as the one that will form the lagging strand template of a potential RF blocked at the rRFB consistent with a previously reported strand-preference of Top1-dependent nicks at the rRFB (19,13). Inversion of the eRFB1 and eRFB2 sequences resulted in an inversion of the Top1cc asymmetry pattern. Together with the S-phase independence of Top1cc formation, this strongly suggests that the eRFB sequence itself directly controls the positioning of the Top1cc (Figure 3C and 3G). The binding of Fob1 and associated proteins to the rRFB may induce a DNA conformation or topology, exposing preferential Top1 cleavage sites (50,51) to Top1.

Despite the Tof2-dependence of Top1ccs at the eRFBs (Figure 3E), we show that the perinuclear anchoring of the rDNA is not maintained at the eRFBs (Figure 2E). Thus, although the rRFB-associated Top1 nicking activity seems to have evolved as a provisional mechanism to normalize topological stress in the rDNA, the nicking itself does not appear to be triggered by rDNA-specific topological conditions, but is mediated directly by the assembly of a Fob1 dependent functional protein complex at the rRFB. As we show here, the formation of the Top1cc at the rRFB requires at least the presence of Fob1 and Tof2. In line with this, Top1 and Tof2 were co-purified with Tap-tagged Fob1 (17) and physical interactions have been reported between Top1 and Tof2 (44). The co-existence of Top1, Tof2 and Fob1 in a complex suggests that these proteins collectively coordinate rDNA transcription, replication and recombination (52) to maintain rDNA stability.

Finally, we show that DNA breaks at the rRFB that were observed on 2D gels (7,11–13) relate to Top1ccs rather than DSBs. The strict S-phase dependency of the DSBs on agarose gels (13) but not of the Top1-dependent nicks (Figure 3B) (19) strongly suggest that these apparent DSBs arise during DNA isolation as a

Downloaded from https://academic.oup.com/nar/article-abstract/42/8/4985/1073375/Reversible-Top1-cleavage-complexes-are-stabilized
by WWZ Bibliothek (Oeffentliche Bibliotherk der UniversitÃ¤t Basel) user
on 10 October 2017

consequence of the experimental melting of the parental duplex DNA between the branch point of a stalled RF and the nearby Top1 nick ahead of the RF. The nick mapped closest to the major RF-pausing site (RFB1) resides only 14 nt ahead of the expected RF (Figure 5A) (13,41), thus generating a relatively unstable duplex region that is likely to melt to generate a DSB fragment even under the mild conditions of DNA isolation used in our and previous experiments (Figure 5A, orange fragment). In contrast, the additional breaks observed in *sgs1*Δ cells—in which RFs pausing at the rRFB are likely to be destabilized and to break more easily—probably reflect canonical DSBs (Figure 5C) (12,14). Importantly, fission yeast *rqh1*^{sgs1} cells, but not wild-type cells, display similar breaks at an ectopic RFB on 1D-gels (53).

Having shown that Top1 is stabilized at the rRFB, we propose a model for how strand-specific DNA nicking by Top1 is achieved. Recruitment to the rRFB complex by interactions with Fob1 and Tof2 (17,44) cannot fully explain the DNA strand and site-specific cleavage. Instead, the DNA structure imposed by wrapping around Fob1 (7), together with a preferential nicking-site sequence and the non-palindromic nature of the Fob1-binding site, might specify the position of Top1 cleavage—bent DNA was indeed shown to be a good substrate for Topoisomerase 1 *in vitro* (54). Following strand incision, Top1cc is stabilized by an rRFB-specific DNA conformation that delays the resealing of the nick (28), contrasting the normally short-lived Top1ccs (Figure 5F). This could be achieved by temporarily displacing the unbound 5′-DNA end from the Top1 catalytic site or from a direct stabilization of the cleavage complex by Fob1, Tof2 or other proteins present at the rRFB (17,44). Importantly, Top1cc stabilization does not require the presence of a pausing RF, but replication through the rRFB will require Top1cc removal to prevent the formation of a DSB. Our data suggest that this removal does not involve excision of Top1, but instead resealing of the nick by Top1 itself. We propose that the ability of Top1cc to complete the reaction and ligate the nick is finally achieved by the disassembly of the proteinaceous complex at the rRFB allowing the passage of the RF. Relieving the torsional stress at the rRFB is especially required assuming rRFB anchoring to the nuclear membrane (Figure 5G). In conclusion, our data not only provide insight into the mechanism of Top1 function in preserving rDNA integrity, but also they might present a general concept for how topoisomerases help at RF impediments.

SUPPLEMENTARY DATA

Supplementary Data are available at NAR Online.

ACKNOWLEDGEMENTS

We thank Serge Boiteux and Michael Lisby for yeast strains and Frank Neumann for plasmids. We are also thankful for Susan M. Gasser's input and support. We thank the Facility for Advanced Imaging and Microscopy from the FMI.

FUNDING

Forschungsfonds of the University of Basel (to O.F. for C.K.) Novartis Research Foundation (to V.D.); Swiss National Science Foundation (to V.D. in SMG's laboratory). Funding for open access charge: University of Basel.

Conflict of interest statement. None declared.

REFERENCES

1. Hill,T.M., Tecklenburg,M.L., Pelletier,A.J. and Kuempel,P.L. (1989) tus, the trans-acting gene required for termination of DNA replication in Escherichia coli, encodes a DNA-binding protein. *Proc. Natl Acad. Sci. USA*., **86**, 1593–1597.
2. Mirkin,E.V. and Mirkin,S.M. (2007) Replication fork stalling at natural impediments. *Microbiol. Mol. Biol. Rev*., **71**, 13–35.
3. Calzada,A., Hodgson,B., Kanemaki,M., Bueno,A. and Labib,K. (2005) Molecular anatomy and regulation of a stable replisome at a paused eukaryotic DNA replication fork. *Gene Dev*., **19**, 1905–1919.
4. Kobayashi,T. and Horiuchi,T. (1996) A yeast gene product, Fob1 protein, required for both replication fork blocking and recombinational hotspot activities. *Genes Cells*., **1**, 465–474.
5. Sogo,J.M., Lopes,M. and Foiani,M. (2002) Fork reversal and ssDNA accumulation at stalled replication forks owing to checkpoint defects. *Science*., **297**, 599–602.
6. Brewer,B.J., Lockshon,D. and Fangman,W.L. (1992) The arrest of replication forks in the rDNA of yeast occurs independently of transcription. *Cell*., **71**, 267–276.
7. Kobayashi,T. (2003) The replication fork barrier site forms a unique structure with Fob1p and inhibits the replication fork. *Mol. Cell Biol*., **23**, 9178–9188.
8. Brewer,B.J. and Fangman,W.L. (1988) A replication fork barrier at the 3′ end of yeast ribosomal RNA genes. *Cell*., **55**, 637–643.
9. Kobayashi,T., Horiuchi,T., Tongaonkar,P., Vu,L. and Nomura,M. (2004) SIR2 regulates recombination between different rDNA repeats, but not recombination within individual rRNA genes in yeast. *Cell*., **117**, 441–453.
10. Kobayashi,T., Heck,D.J., Nomura,M. and Horiuchi,T. (1998) Expansion and contraction of ribosomal DNA repeats in *Saccharomyces cerevisiae*: requirement of replication fork blocking (Fob1) protein and the role of RNA polymerase I. *Gene Dev*., **12**, 3821–3830.
11. Weitao,T., Budd,M., Hoopes,L. and Campbell,J. (2003) Dna2 helicase/nuclease causes replicative fork stalling and double-strand breaks in the ribosomal DNA of Saccharomyces cerevisiae. *J. Biol. Chem*., **278**, 22513–22522.
12. Weitao,T., Budd,M. and Campbell,J.L. (2003) Evidence that yeast SGS1, DNA2, SRS2, and FOB1 interact to maintain rDNA stability. *Mut. Res*., **532**, 157–172.
13. Burkhalter,M.D. and Sogo,J.M. (2004) rDNA enhancer affects replication initiation and mitotic recombination: Fob1 mediates nucleolytic processing independently of replication. *Mol. Cell*., **15**, 409–421.
14. Fritsch,O., Burkhalter,M.D., Kais,S., Sogo,J.M. and Schär,P. (2010) DNA ligase 4 stabilizes the ribosomal DNA array upon fork collapse at the replication fork barrier. *DNA Repair*., **9**, 879–888.
15. Mekhail,K., Seebacher,J., Gygi,S.P. and Moazed,D. (2008) Role for perinuclear chromosome tethering in maintenance of genome stability. *Nature*., **456**, 667–670.
16. Chan,J.N.Y., Poon,B.P.K., Salvi,J., Olsen,J.B., Emili,A. and Mekhail,K. (2011) Perinuclear cohibin complexes maintain replicative life span via roles at distinct silent chromatin domains. *Dev. Cell*., **20**, 867–879.
17. Huang,J., Brito,I.L., Villen,J., Gygi,S.P., Amon,A. and Moazed,D. (2006) Inhibition of homologous recombination by a

Downloaded from https://academic.oup.com/nar/article-abstract/42/8/4985/1073375/Reversible-Top1-cleavage-complexes-are-stabilized
by WWZ Bibliothek (Oeffentliche Bibliotherk der UniversitÃ¤t Basel) user
on 10 October 2017

cohesin-associated clamp complex recruited to the rDNA recombination enhancer. *Gene Dev.*, **20**, 2887–2901.
18. French,S.L., Sikes,M.L., Hontz,R.D., Osheim,Y.N., Lambert,T.E., Hage,El,A., Smith,M.M., Tollervey,D., Smith,J.S. and Beyer,A.L. (2011) Distinguishing the roles of Topoisomerases I and II in relief of transcription-induced torsional stress in yeast rRNA genes. *Mol. Cell Biol.*, **31**, 482–494.
19. Vogelauer,M. and Camilloni,G. (1999) Site-specific in vivo cleavages by DNA topoisomerase I in the regulatory regions of the 35S rRNA in Saccharomyces cerevisiae are transcription independent. *J. Mol. Biol.*, **293**, 19–28.
20. Brill,S.J., DiNardo,S., Voelkel-Meiman,K. and Sternglanz,R. (1987) Need for DNA topoisomerase activity as a swivel for DNA replication for transcription of ribosomal RNA. *Nature.*, **326**, 414–416.
21. Schultz,M.C., Brill,S.J., Ju,Q., Sternglanz,R. and Reeder,R.H. (1992) Topoisomerases and yeast rRNA transcription: negative supercoiling stimulates initiation and topoisomerase activity is required for elongation. *Gene Dev.*, **6**, 1332–1341.
22. Bryk,M., Banerjee,M., Murphy,M., Knudsen,K.E., Garfinkel,D.J. and Curcio,M.J. (1997) Transcriptional silencing of Ty1 elements in the RDN1 locus of yeast. *Gene Dev.*, **11**, 255–269.
23. Smith,J.S. and Boeke,J.D. (1997) An unusual form of transcriptional silencing in yeast ribosomal DNA. *Gene Dev.*, **11**, 241–254.
24. Smith,J.S., Caputo,E. and Boeke,J.D. (1999) A genetic screen for ribosomal DNA silencing defects identifies multiple DNA replication and chromatin-modulating factors. *Mol. Cell Biol.*, **19**, 3184–3197.
25. Christman,M.F., Dietrich,F.S. and Fink,G.R. (1988) Mitotic recombination in the rDNA of S. cerevisiae is suppressed by the combined action of DNA topoisomerases I and II. *Cell.*, **55**, 413–425.
26. Kim,R.A. and Wang,J.C. (1989) A subthreshold level of DNA topoisomerases leads to the excision of yeast rDNA as extrachromosomal rings. *Cell.*, **57**, 975–985.
27. Zhu,J. and Schiestl,R.H. (2004) Human topoisomerase I mediates illegitimate recombination leading to DNA insertion into the ribosomal DNA locus in Saccharomyces cerevisiae. *Mol. Genet. Genom.*, **271**, 347–358.
28. Koster,D.A., Croquette,V., Dekker,C., Shuman,S. and Dekker,N.H. (2005) Friction and torque govern the relaxation of DNA supercoils by eukaryotic topoisomerase IB. *Nature.*, **434**, 671–674.
29. Champoux,J.J. (2011) Human DNA Topoisomerase I: Structure, Enzymology and Biology. *DNA Topoisomerases and Cancer*. Springer New York, New York, NY, pp. 53–69.
30. Rohner,S., Gasser,S.M. and Meister,P. (2008) Modules for cloning-free chromatin tagging in Saccharomyces cerevisae. *Yeast.*, **25**, 235–239.
31. van Attikum,H., Fritsch,O., Hohn,B. and Gasser,S.M. (2004) Recruitment of the INO80 complex by H2A phosphorylation links ATP-dependent chromatin remodeling with DNA double-strand break repair. *Cell.*, **119**, 777–788.
32. Martin,S.G., Laroche,T., Suka,N., Grunstein,M. and Gasser,S.M. (1999) Relocalization of telomeric Ku and SIR proteins in response to DNA strand breaks in yeast. *Cell.*, **97**, 621–633.
33. Takahashi,T., Burguiere-Slezak,G., Van der Kemp,P.A. and Boiteux,S. (2011) Topoisomerase 1 provokes the formation of short deletions in repeated sequences upon high transcription in Saccharomyces cerevisiae. *Proc. Natl Acad. Sci. USA.*, **108**, 692–697.
34. Dion,V., Kalck,V., Horigome,C., Towbin,B.D. and Gasser,S.M. (2012) Increased mobility of double-strand breaks requires Mec1, Rad9 and the homologous recombination machinery. *Nat. Cell Biol.*, **14**, 502–509.
35. Meister,P., Gehlen,L.R., Varela,E., Kalck,V. and Gasser,S.M. (2010) Visualizing yeast chromosomes and nuclear architecture. *Meth. Enzymol.*, **470**, 535–567.
36. Neumann,F.R., Dion,V., Gehlen,L.R., Tsai-Pflugfelder,M., Schmid,R., Taddei,A. and Gasser,S.M. (2012) Targeted INO80 enhances subnuclear chromatin movement and ectopic homologous recombination. *Gene Dev.*, **26**, 369–383.
37. Ponti,A., Schwarb,P., Gulati,A. and Bäker,V. (2007) Huygens remote manager: a web interface for high-volume batch deconvolution. *Imag. Microscop.*, **9**, 57–58.
38. Huang,J. and Moazed,D. (2003) Association of the RENT complex with nontranscribed and coding regions of rDNA and a regional requirement for the replication fork block protein Fob1 in rDNA silencing. *Gene Dev.*, **17**, 2162–2176.
39. Nieduszynski,C.A., Hiraga,S.-I., Ak,P., Benham,C.J. and Donaldson,A.D. (2007) OriDB: a DNA replication origin database. *Nucleic Acids Res.*, **35**, D40–D46.
40. Torres-Rosell,J., Sunjevaric,I., De Piccoli,G., Sacher,M., Eckert-Boulet,N., Reid,R., Jentsch,S., Rothstein,R., Aragón,L. and Lisby,M. (2007) The Smc5-Smc6 complex and SUMO modification of Rad52 regulates recombinational repair at the ribosomal gene locus. *Nat. Cell Biol.*, **9**, 923–931.
41. Di Felice,F., Cioci,F. and Camilloni,G. (2005) FOB1 affects DNA topoisomerase I in vivo cleavages in the enhancer region of the Saccharomyces cerevisiae ribosomal DNA locus. *Nucleic Acids Res.*, **33**, 6327–6337.
42. Vance,J.R. and Wilson,T.E. (2002) Yeast Tdp1 and Rad1-Rad10 function as redundant pathways for repairing Top1 replicative damage. *Proc. Natl Acad. Sci. USA.*, **99**, 13669–13674.
43. Liu,C., Pouliot,J.J. and Nash,H.A. (2002) Repair of topoisomerase I covalent complexes in the absence of the tyrosyl-DNA phosphodiesterase Tdp1. *Proc. Natl Acad. Sci. USA.*, **99**, 14970–14975.
44. Park,H. and Sternglanz,R. (1999) Identification and characterization of the genes for two topoisomerase I-interacting proteins from Saccharomyces cerevisiae. *Yeast.*, **15**, 35–41.
45. Christman,M.F., Dietrich,F.S., Levin,N.A., Sadoff,B.U. and Fink,G.R. (1993) The rRNA-encoding DNA array has an altered structure in topoisomerase I mutants of Saccharomyces cerevisiae. *Proc. Natl Acad. Sci. USA.*, **90**, 7637–7641.
46. Ii,M., Ii,T. and Brill,S.J. (2007) Mus81 functions in the quality control of replication forks at the rDNA and is involved in the maintenance of rDNA repeat number in *Saccharomyces cerevisiae*. *Mut. Res.*, **625**, 1–19.
47. Versini,G., Comet,I., Wu,M., Hoopes,L., Schwob,E. and Pasero,P. (2003) The yeast Sgs1 helicase is differentially required for genomic and ribosomal DNA replication. *EMBO J.*, **22**, 1939–1949.
48. Defossez,P.A., Prusty,R., Kaeberlein,M., Lin,S.J., Ferrigno,P., Silver,P.A., Keil,R.L. and Guarente,L. (1999) Elimination of replication block protein Fob1 extends the life span of yeast mother cells. *Mol. Cell.*, **3**, 447–455.
49. Johzuka,K. and Horiuchi,T. (2002) Replication fork block protein, Fob1, acts as an rDNA region specific recombinator in S. cerevisiae. *Genes Cells.*, **7**, 99–113.
50. Shuman,S. and Prescott,J. (1990) Specific DNA cleavage and binding by vaccinia virus DNA topoisomerase I. *J. Biol. Chem.*, **265**, 17826–17836.
51. Edwards,K.A., Halligan,B.D., Davis,J.L., Nivera,N.L. and Liu,L.F. (1982) Recognition sites of eukaryotic DNA topoisomerase I: DNA nucleotide sequencing analysis of topo I cleavage sites on SV40 DNA. *Nucleic Acids Res.*, **10**, 2565–2576.
52. Tsang,E. and Carr,A.M. (2008) Replication fork arrest, recombination and the maintenance of ribosomal DNA stability. *DNA Repair.*, **7**, 1613–1623.
53. Ahn,J., Osman,F. and Whitby,M. (2005) Replication fork blockage by RTS1 at an ectopic site promotes recombination in fission yeast. *EMBO J.*, **24**, 2011–2023.
54. Caserta,M., Amadei,A., Di Mauro,E. and Camilloni,G. (1989) In vitro preferential topoisomerization of bent DNA. *Nucleic Acids Res.*, **17**, 8463–8474.

Downloaded from https://academic.oup.com/nar/article-abstract/42/8/4985/1073375/Reversible-Top1-cleavage-complexes-are-stabilized
by WWZ Bibliothek (Oeffentliche Bibliotherk der UniversitÃ¤t Basel) user
on 10 October 2017